

Supplementary Material

Cytochrome P450 enzyme-mediated auto-enhanced photodynamic cancer therapy of co-nanoassembly between clopidogrel and photosensitizer

Authors: Qiu Wang^{a,1}, Mengchi Sun^{a,1}, Dan Li^a, Chang Li^a, Cong Luo^a, Zhaomeng Wang^a, Wenjuan Zhang^a, Zimeng Yang^a, Yao Feng^b, Shuang Wang^c, Zhonggui He^a, Haotian Zhang^d, Qiming Kan^d, Wei Sun^{e,*}, Jin Sun^{a,*}

Affiliations:

¹Both authors contributed equally

^aWuya College of Innovation, Shenyang Pharmaceutical University, Shenyang, 110016, P. R. China

^bKey Laboratory of Structure-Based Drug Design and Discovery, Ministry of Education, Shenyang Pharmaceutical University, Shenyang, 110016, P. R. China

^cSchool of Pharmacy, Shenyang Pharmaceutical University, Shenyang, 110016, P. R. China

^dSchool of Life Science and Biopharmaceutics, Shenyang Pharmaceutical University, Shenyang, 110016, P. R. China

^eCollege of Medical Device, Shenyang Pharmaceutical University, Shenyang, 110016,

P. R. China

***Corresponding Author:**

Prof. Jin Sun Ph.D

Wuya College of Innovation, Shenyang Pharmaceutical University, Shenyang,
Liaoning, 110016, P. R. China

Tel/Fax: +86-24-23986321

E-mail: sunjin@sypu.edu.cn

Dr. Wei Sun

College of Medical Device, Shenyang Pharmaceutical University, Shenyang, Liaoning,
110016, P. R. China

Tel: +86-24-43520356

E-mail: sunwei19801208@163.com

Table S1. Optimization of molar ratios of CPG to PPa

Molar ratios of CPG to PPa	Z-Average (d. nm)	PDI	CI (50% inhibition)
1:5	120.3 ± 6.704	0.240 ± 0.032	3.1
1:2	126.3 ± 3.915	0.257 ± 0.057	3.7
1:1	91.17 ± 4.682	0.268 ± 0.039	3.8
2:1	141.9 ± 4.884	0.119 ± 0.069	0.57
5:1	268.3 ± 8.130	0.165 ± 0.144	0.86

Table S2. Pharmacokinetic parameters of PPa from CPG/PPa mixture, non-PEGylated CPG/PPa

NPs and CPG/PPa NPs (n=3).

Formulations	AUC ₀₋₁₂ (nmol h/mL)	t _{1/2} (h)
CPG/PPa mixture	87.408 ± 4.360	4.93 ± 0.442
non-PEGylated CPG/PPa NPs	117.2 ± 15.055	4.813 ± 0.704
CPG/PPa NPs	177.561 ± 9.648	5.9 ± 1.202

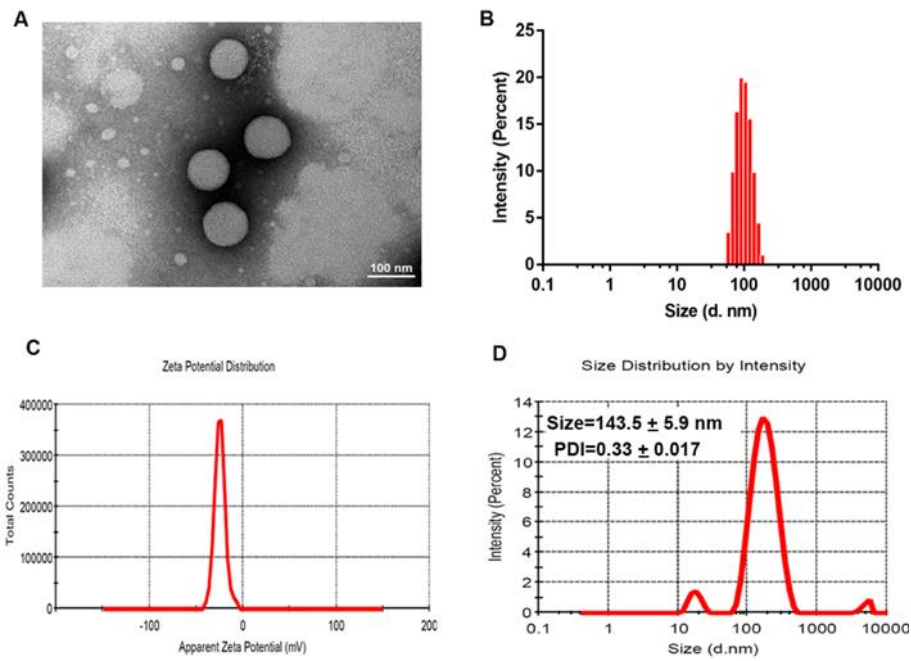


Figure S1. The characterization of non-PEGylated CPG/PPa NPs. (A) TEM image. (B) Intensity distribution profile of size. (C) The zeta potential of non-PEGylated CPG/PPa NPs. (D) Intensity distribution of non-PEGylated CPG/PPa NPs after incubation with PBS including 10% FBS for 4 h.

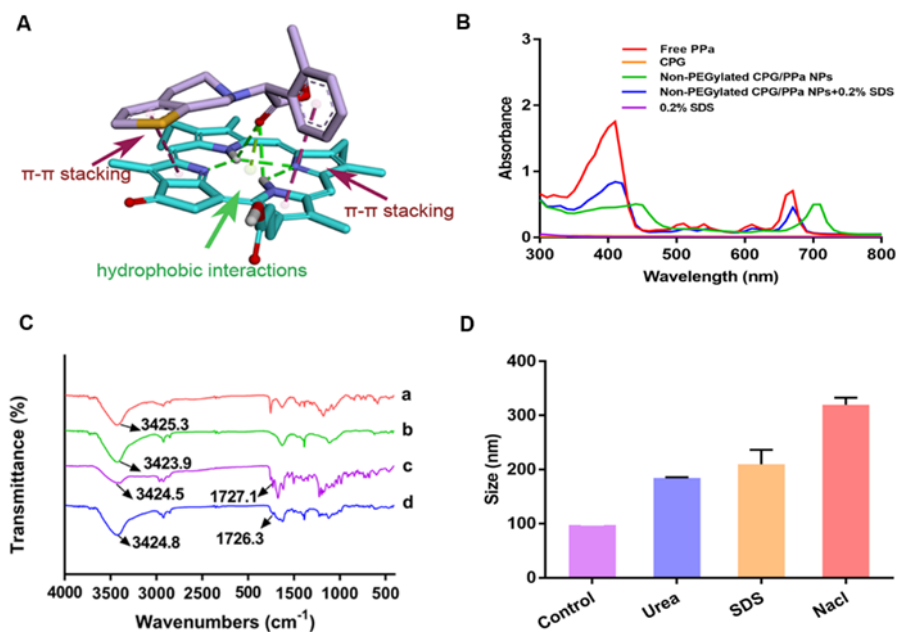


Figure S2. The co-assembly mechanism of non-PEGylated CPG/PPa NPs. (A) Molecular dynamics simulations of CPG and PPa molecules. (B) The UV absorption of free PPa, CPG, non-PEGylated CPG/PPa NPs, non-PEGylated CPG/PPa NPs+0.2% SDS, 0.2% SDS. (C) The FT-IR spectra of CPG (a), CPG/PPa NPs (without pegylation) (b), CPG/PPa mixture (c), and PPa (d). (D) The size change of non-PEGylated CPG/PPa NPs treated with urea, SDS and NaCl (200 mM).

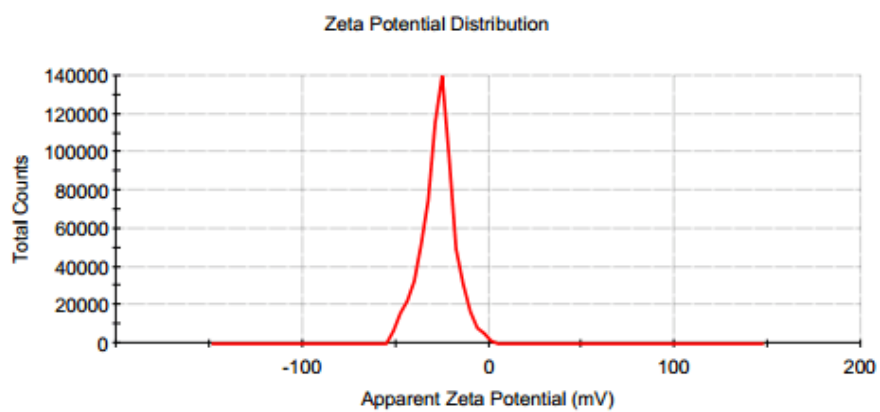


Figure S3. Zeta potential of CPG/PPa NPs.

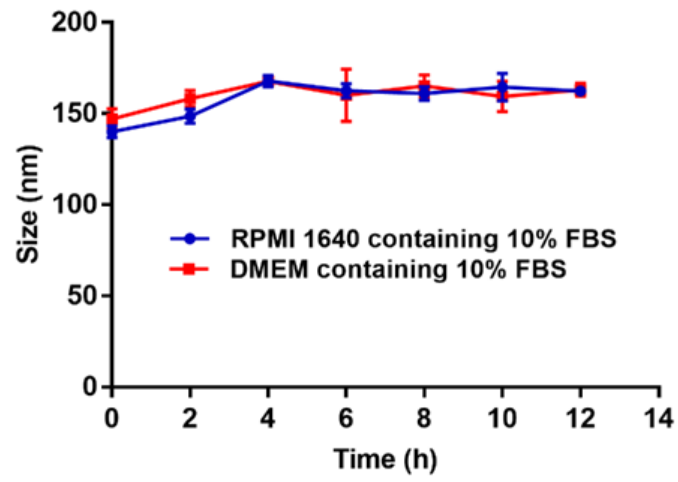


Figure S4. The stability of CPG/PPa NPs incubated in RPMI 1640 and DMEM medium containing 10% FBS for 12 h (n=3).

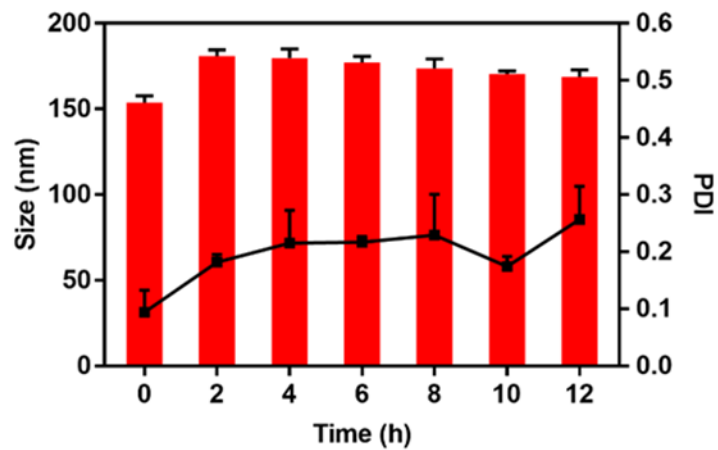


Figure S5. The colloidal stability of CPG/PPa NPs in plasma (n=3).

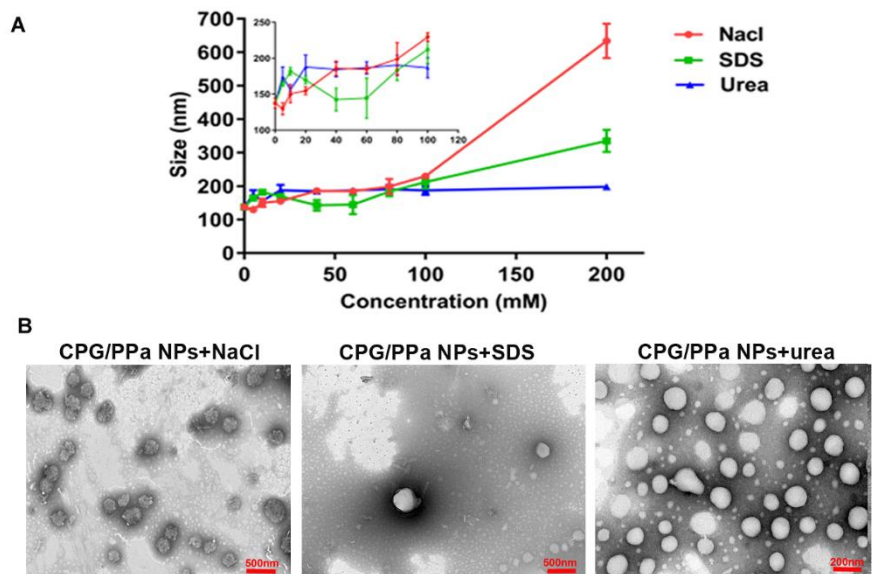


Figure S6. (A) The size changes of CPG/PPa NPs after treatment with different concentrations of NaCl, SDS, and urea, respectively. (B) The TEM images of CPG/PPa NPs treated with NaCl, SDS and urea (100 mM).

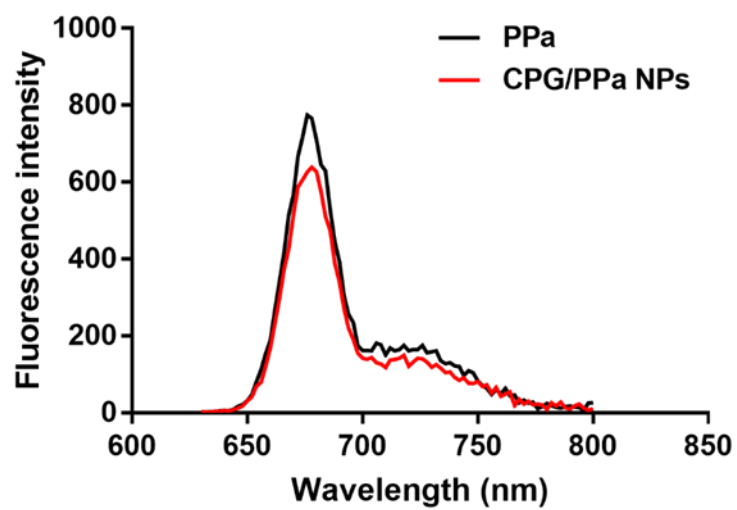


Figure S7. The PPa fluorescence spectra of free PPa and CPG/PPa NPs.

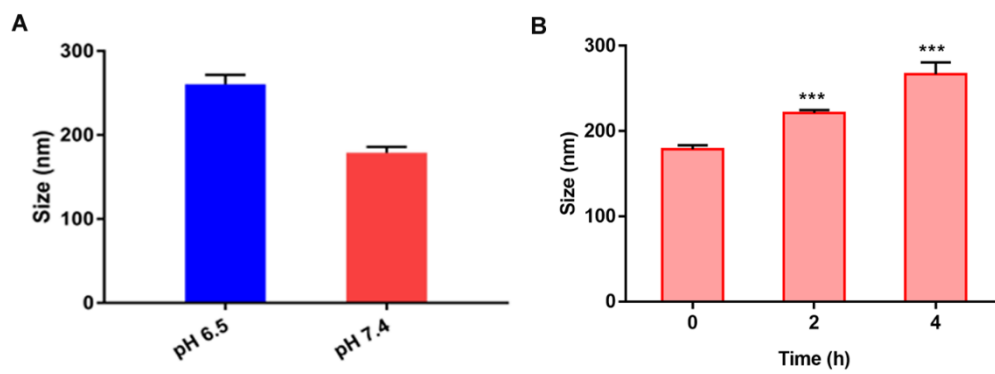


Figure S8. (A) The size changes of CPG/PPa NPs after treatment with different pH (n=3). (B) The stability of the CPG/PPa NPs in solution with pH 6.5 (n=3, ***P < 0.001).

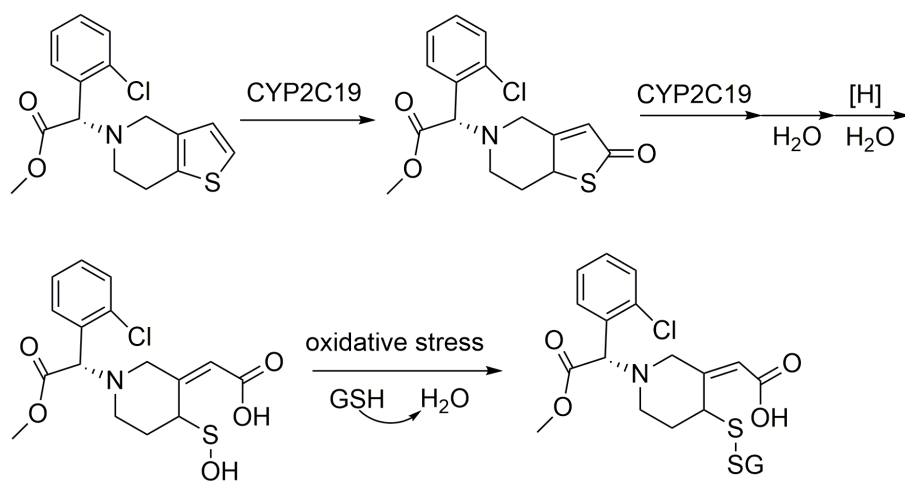


Figure S9. Metabolic pathway of CPG.

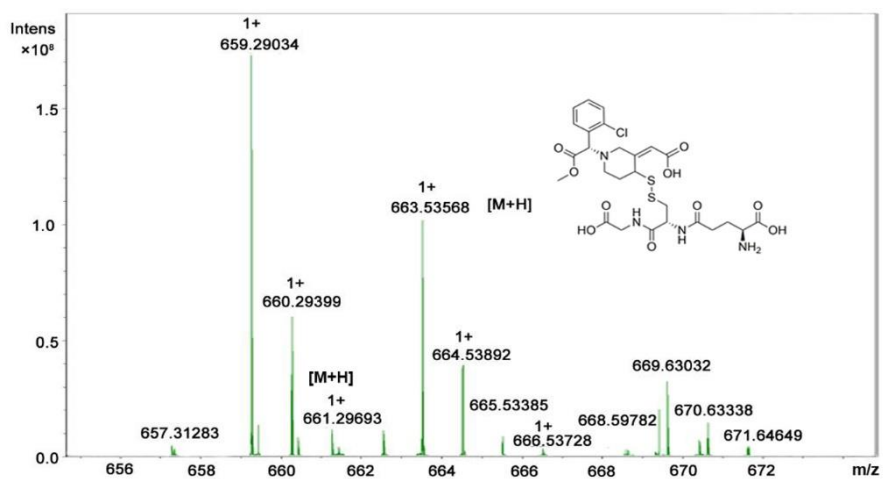


Figure S10. Mass spectrum of the GPG-SS-GSH.

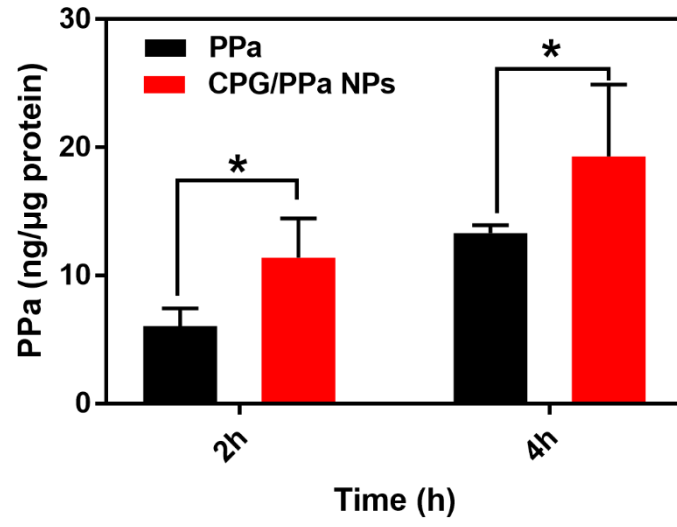


Figure S11. Quantitative analysis of cellular uptake of free PPa and CPG/PPa NPs at 2 h and 4 h.

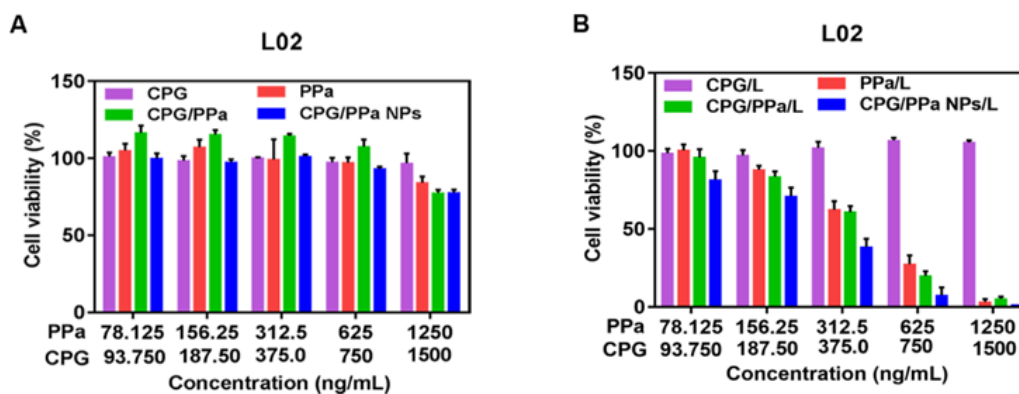


Figure S12. The cell viability of CPG, PPa, CPG/PPa mixture and CPG/PPa NPs against L02 cells with or without laser irradiation (n=3). (A) Without laser irradiation. (B) With irradiation (660nm, 30 mW/cm² for 2 min).

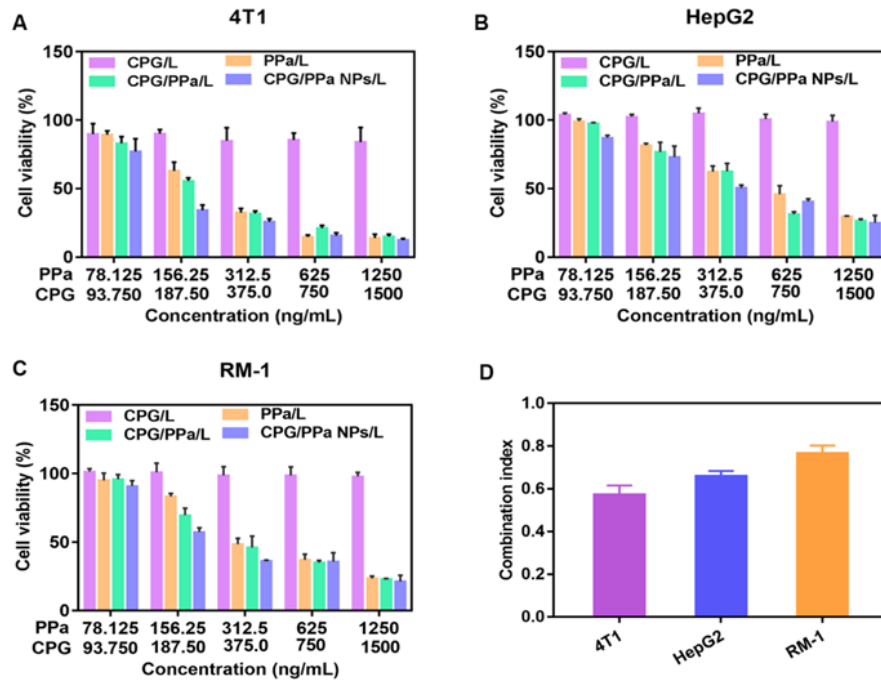


Figure S13. *In vitro* cell viability of CPG, PPa, CPG/PPa mixture and CPG/PPa NPs against 4T1, HepG2 and RM-1 cells incubated with GSH-OEt under laser irradiation (n=3). (A) 4T1 cells, (B) HepG2 cells, (C) RM-1 cells. (D) The combination index (50% inhibition) of CPG/PPa NPs in 4T1, HepG2 and RM-1 cells.

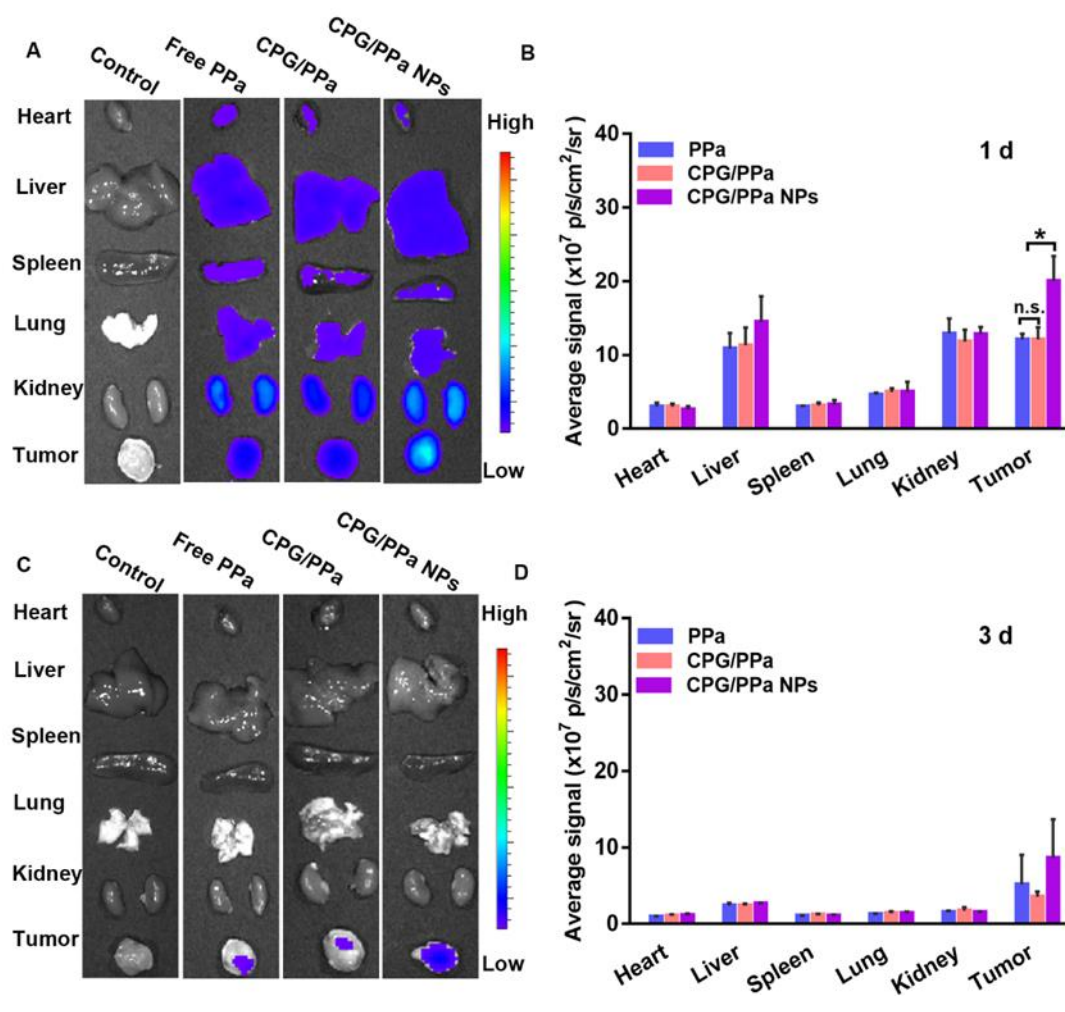


Figure S14. The biodistribution of PBS, free PPa, CPG/PPa and CPG/PPa NPs in 4T1 tumor-bearing BALB/c mice. (A) *In vitro* fluorescence imaging of major organs and tumors at 1 d, (B) Quantitative analysis average fluorescence intensity at 1 d; (C) *In vitro* fluorescence imaging of major organs and tumors at 3 d; (D) Quantitative analysis average fluorescence intensity at 3 d (n = 3, n.s. no significance, *P < 0.05,).

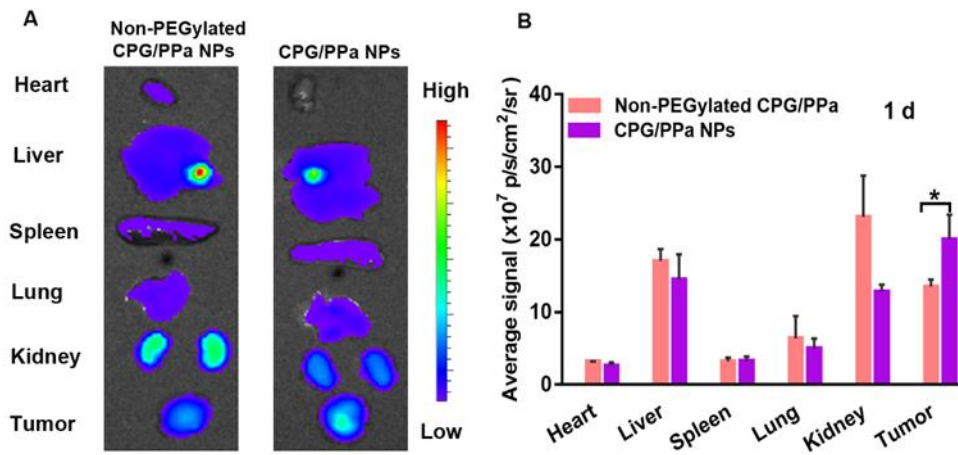


Figure S15. The biodistribution of non-PEGylated CPG/PPa NPs and CPG/PPa NPs in 4T1 tumor-bearing BALB/c mice at post 1 d administration. (A) *In vitro* fluorescence imaging of major organs and tumors, (B) Quantitative analysis average fluorescence intensity (n = 3, *P < 0.05).

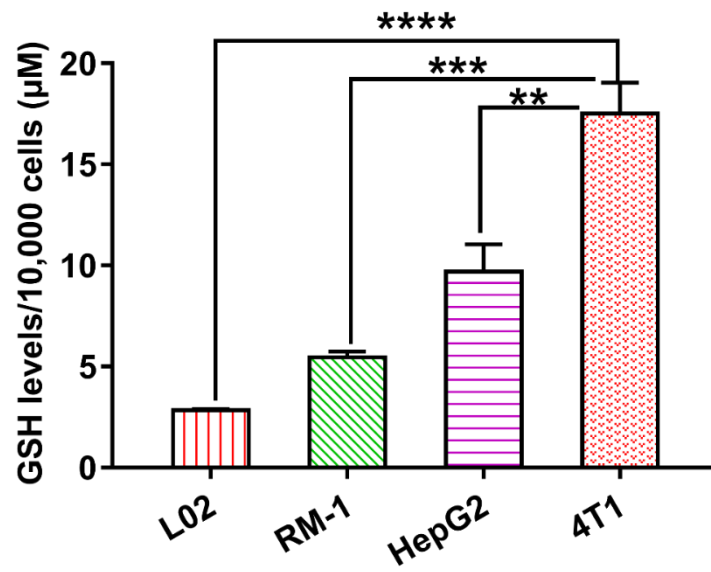


Figure S16. The GSH levels of L02, RM-1, HepG2, and 4T1.

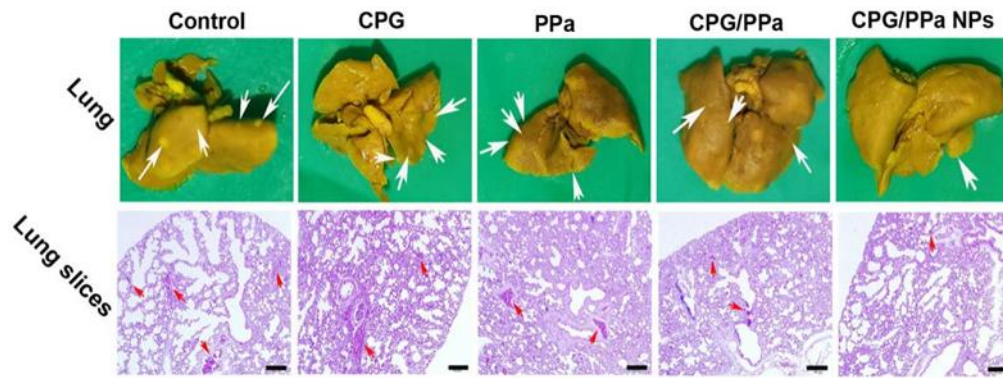


Figure S17. Images of picric acid staining of lungs and H&E staining of the lung slices prepared from different administration groups after treatments.

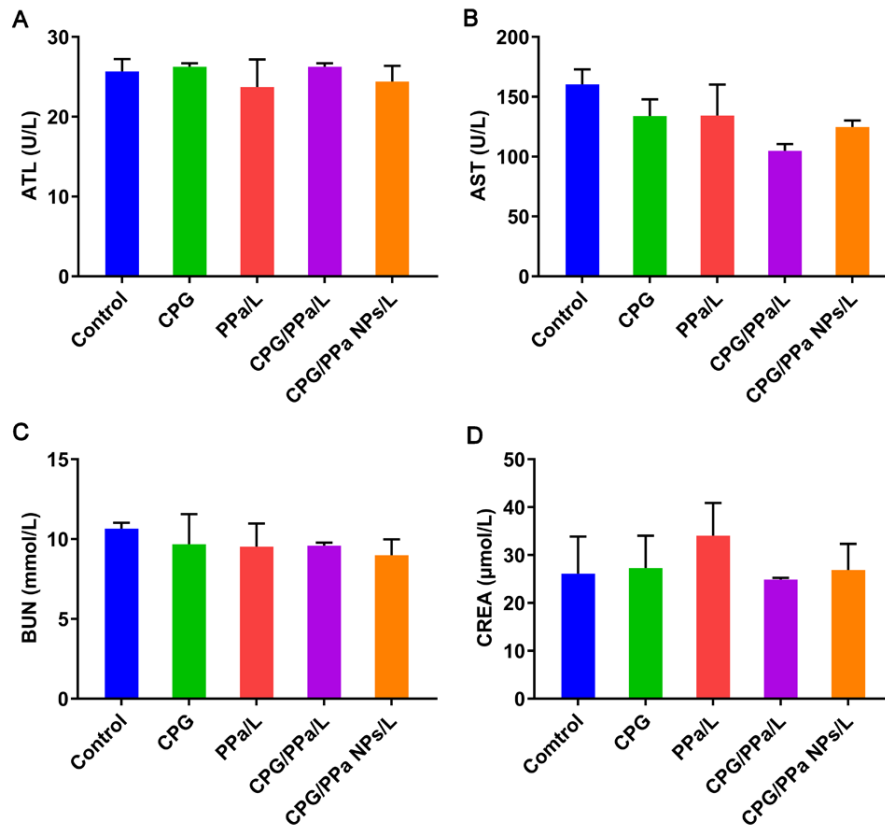


Figure S18. Hepatic and renal function parameters after the last treatment. (A) ALT: alanine aminotransferase; (B) AST: aspartate aminotransferase; (C) BUN: blood urea nitrogen; (D) CREA: creatinine. (n=3)

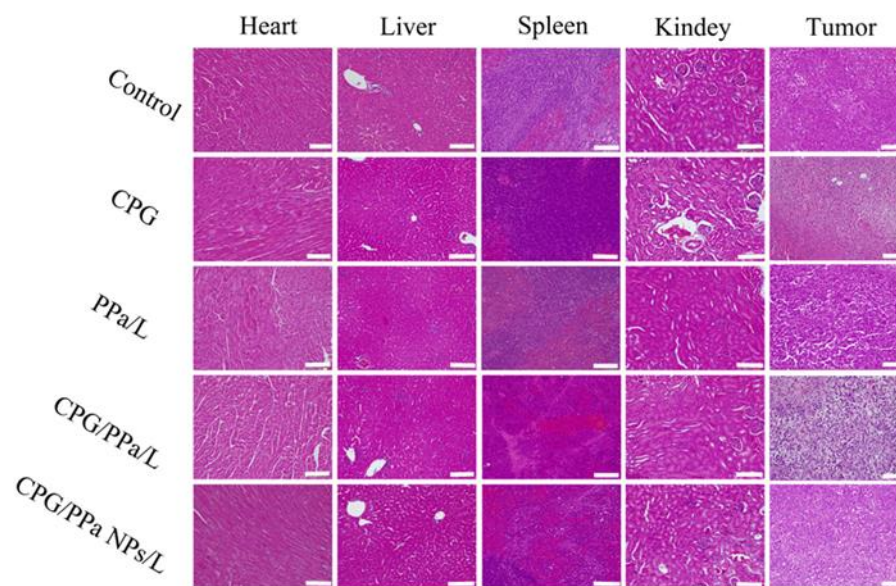


Figure S19. H&E staining of the major organs and tumors after treatments. Scale bar represents 100 μ m.

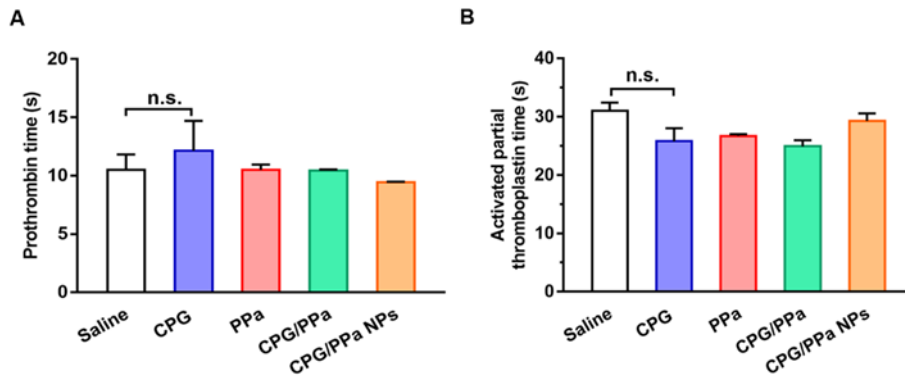


Figure S20. The coagulation indicators after last treatment. (A) Prothrombin time (PT). (B) Activated partial thromboplastin time (APTT).